

Nucleon-antinucleon interaction from the Skyrme model

Yang Lu and R. D. Amado

Department of Physics, University of Pennsylvania, Philadelphia, Pennsylvania 19104

(Received 3 June 1996)

We calculate the nucleon-antinucleon static potential in the Skyrme model using the product ansatz and including some finite N_C (number of colors) corrections. The mid- and long-range part of the spin-spin and tensor force are mostly correctly given in both isospin channels while the central interaction has insufficient midrange attraction. This is a well-known problem of the product ansatz that should be repaired with better Skyrme dynamics. [S0556-2813(96)06810-0]

PACS number(s): 13.75.Cs, 11.80.Gw

I. INTRODUCTION

The Skyrme model [1] is an example of what QCD might look like in the classical or large number of colors (N_C) limit [2,3]. The dynamics of the $SU(2)$ Skyrme model is carried purely by a classical pion field. Hadrons appear as topological solitons in this nonlinear meson field theory. These are the appropriate degrees of freedom for the nonperturbative, long wavelength limit of QCD, and hence for low energy baryon and pion physics. The Skyrme model has been applied to the nucleon static properties [4] and the nucleon-nucleon interactions [5–8] with reasonable success. In the past few years, nucleon annihilation has been investigated from the Skyrme point of view. Sommermann *et al.* [9] studied the dynamics of ungroomed Skyrminion-anti-Skyrminion (SS) collisions. They found that annihilation proceeds quickly with the creation of a coherent pion pulse. This was confirmed by Shao, Walet, and Amado [10]. The notion that annihilation leads to an intense coherent pion field burst gives reason for considering annihilation within the classical Skyrme approach. The idea, that the annihilation products, pion and other mesons, come from a coherent wave of meson fields arising from soliton-antisoliton dynamics, turns out to be very fruitful [11,12]. Experimental data such as annihilation branching ratios among meson types and pion charge types from low energy annihilation are well explained with minimal parameters [12]. Furthermore this picture provides a unified view of annihilation in which all the channels come from a single process.

Previous studies of annihilation in the Skyrme context, with the exception of [9], have concentrated on the final state mesons. A full account of the process requires a description of the initial state nucleon-antinucleon interaction and of the dynamics leading up to annihilation as well. In this paper, as a first step in that direction, we extend the application of the Skyrme model to the interaction of $N\bar{N}$ in the product ansatz. (We note that the energy of SS in the product ansatz was studied for two configurations by Musakhanov and Musatov [13].) Phenomenologically, the $N\bar{N}$ potential is not as well established as the NN potential. At distances less than one fermi, the interaction is dominated by annihilation. However, at larger distances, a meaningful potential can be defined and studied either by G transformation on the NN meson exchange potential or phenomenologically. Here we will com-

pare our Skyrme model results to this phenomenology. We will see that at large distance, where the product ansatz makes the best sense, the potentials we find agree qualitatively and, in most cases, quantitatively with phenomenological interactions. At intermediate and short distances, we do less well, but at these distances the product ansatz is not valid. However, it is still suggestive. To obtain the interaction at intermediate distances, we would need to study the full Skyrme dynamics at these distances. For the static $S\bar{S}$ this is somewhat more complex than in the corresponding SS case studied by Walhout and Wambach [14], but is possible and we plan to return to it. The full, time dependent, dynamical $S\bar{S}$ problem is far more difficult than the SS case and is plagued for $S\bar{S}$ by numerical instabilities [9,15]. For all these reasons, and because this paper is a first step, we begin by exploring the static interaction in the product ansatz. In order to carry out our study it is necessary to include Δ and $\bar{\Delta}$ mixing in the potential as was first suggested in the NN case [8,16]. We do not even attempt to study the spin-orbit interaction or other nonstatic forces since these are notoriously difficult to calculate in the Skyrme approach [17,18].

In the context of the product ansatz, we find that the ungroomed $S\bar{S}$ channel studied in [9] is the most attractive channel and that it leads to rapid annihilation. For nonzero grooming, we find that the $S\bar{S}$ interaction can be repulsive. Therefore it seems likely that the dynamics in groomed channels could be very different from that exhibited in [9]. Since the physical nucleon is represented by an average over differently groomed Skyrminions, annihilation in the nucleon-antinucleon system may proceed more slowly than that of ungroomed $S\bar{S}$.

In Sec. II we study the interaction energy of $S\bar{S}$ as a function of separation and relative grooming in the product ansatz. We start by studying the very simplified case of Skyrminion and groomed anti-Skyrminion on top of each other. This is a physically artificial case, but it permits analytic evaluation and teaches us something, albeit qualitative, about the dependence of the $S\bar{S}$ interaction on grooming. We find that for zero separation and zero grooming, the $S\bar{S}$ system has zero total energy, as we expect. This is the case of complete annihilation. However, at relative grooming angle of π , and still zero separation, the product ansatz gives a total energy

for the $S\bar{S}$ system of four times the single Skyrmion energy, corresponding to a very repulsive interaction. This clearly indicates that the $S\bar{S}$ interaction is a strong function of relative grooming. Next we study, always in the product ansatz, the interaction energy of $S\bar{S}$ at nonzero separation as a function of grooming. We project to the nucleon space by the algebraic methods of [19] which also include finite N_C corrections. In Sec. III we consider the effects of rotational excitations by including intermediate states with Δ and $\bar{\Delta}$. We first evaluate the corrections to the $N\bar{N}$ potential in perturbation theory and then study the effect fully by diagonalizing in the space spanned by N , Δ , and corresponding antiparticles. Our results are presented in Sec. IV.

II. THE INTERACTION ENERGY IN THE $S\bar{S}$ SYSTEM AS A FUNCTION OF SEPARATION AND RELATIVE GROOMING

A. The case of an S on top of a groomed \bar{S}

We calculate the energy of the Skyrmion and anti-Skyrmion system using the Skyrme Lagrangian. The density of this Lagrangian is given by

$$\mathcal{L} = \frac{f_\pi^2}{4} \text{Tr}(\partial_\mu U \partial^\mu U^\dagger) + \frac{1}{32e^2} \text{Tr}(Q_{\mu\nu} Q^{\mu\nu\dagger}) + \frac{f_\pi^2}{2} m_\pi^2 \text{Tr}(U - 1), \quad (1)$$

where U is a unitary SU(2) valued field and

$$Q_{\mu\nu} = [(\partial_\mu U)U^\dagger, (\partial_\nu U)U^\dagger]. \quad (2)$$

The first term in the Lagrangian comes from the nonlinear σ model and the second is the Skyrme term. The third term is a pion mass term and we take $m_\pi = 139$ MeV. We take the parameters in the Lagrangian to have the values $f_\pi = 93$ MeV and $e = 4.76$ [14]. These values guarantee that the long distance tail of the nucleon-antinucleon interaction will agree with phenomenology, by virtue of the Goldberger-Treiman relation.¹

We begin by studying the energy in the product ansatz for the case of zero separation. We include the first two terms in the Lagrangian. The mass term is neglected since it does not lead to additional understanding of this simple configuration. Let $U = \exp(i\boldsymbol{\tau} \cdot \hat{r} F(r))$ be the ungroomed Skyrme SU(2) field. The ungroomed \bar{S} would be U^\dagger . The rotation or grooming matrix C on \bar{S} is

$$C = \cos(\beta/2) + i\boldsymbol{\tau} \cdot \hat{n} \sin(\beta/2). \quad (3)$$

¹There is always a conflict in the Skyrme approach between choosing f_π and e to give the correct nucleon and delta masses or to give the correct strength of the pion tail. Since we are concentrating on the $N\bar{N}$ interaction here we follow [14] and choose the parameters for the pion tail. This latitude is a measure of the arbitrariness of the Skyrme approach and is intrinsic to it.

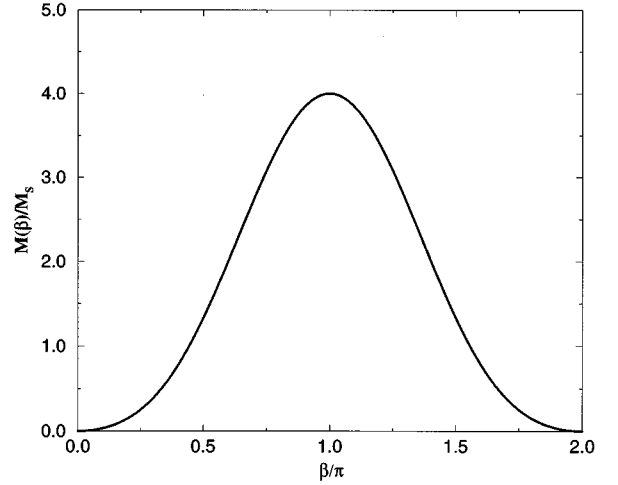


FIG. 1. Mass of the $S\bar{S}$ at zero separation and with relative grooming angle β . M_S is the Skyrmion mass.

This corresponds to a grooming rotation through angle β about the \hat{n} axis. The product ansatz with this relative grooming is

$$U_{\text{PA}} = U C U^\dagger C^\dagger. \quad (4)$$

Note that the energy is a function of only the relative grooming and should be zero with no grooming (since for $\beta=0$, $U_{\text{PA}}=1$).

The energy density is

$$E = -\frac{1}{4} \text{tr} \mathcal{L}_i \mathcal{L}_i - \frac{1}{32} \text{tr} [\mathcal{L}_i, \mathcal{L}_j]^2 \quad (5)$$

in Skyrme units [energy in f_π/e and length in $1/(ef_\pi)$]. The chiral (left-handed) derivative is

$$\mathcal{L}_i = U_{\text{PA}}^\dagger \partial_i U_{\text{PA}}. \quad (6)$$

Suppose for the Skyrme chiral angle $F(r)$, the mass contribution to the $B=1$ Skyrmion from the nonlinear σ -model term is M_2 and from the Skyrme term M_4 . After some algebra, we arrive at the following result for the total energy of the $S\bar{S}$ product ansatz at relative grooming angle β and zero separation:

$$M_{S\bar{S}}(\beta) = \frac{8}{3} \sin^2\left(\frac{\beta}{2}\right) M_2 + \frac{16}{3} \sin^4\left(\frac{\beta}{2}\right) M_4. \quad (7)$$

For the profile $F(r)$ which minimizes the $B=1$ Skyrme mass, we have $M_2 = M_4 = M/2$ from scaling arguments. Here M is the mass of the Skyrmion. We then have

$$M_{S\bar{S}}(\beta)/M = \frac{4}{3} \sin^2\left(\frac{\beta}{2}\right) \left[1 + 2 \sin^2\left(\frac{\beta}{2}\right) \right], \quad (8)$$

which is plotted in Fig. 1.

The maximum occurs at $\beta = \pi$, the maximum grooming, with the value $4M$. This indicates that the $S\bar{S}$ is quite repulsive at this setting. Of course for $\beta=0$ or 2π , the total

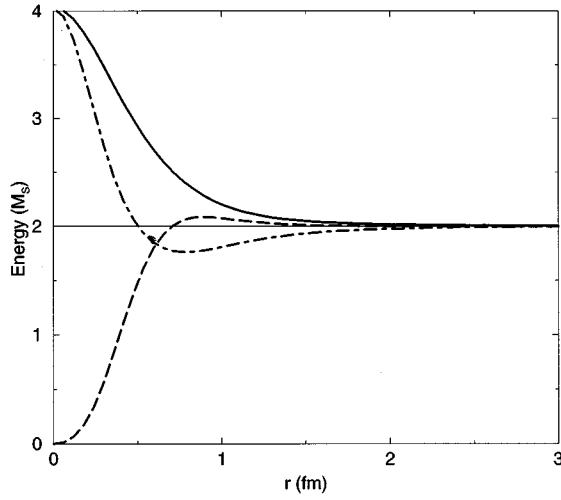


FIG. 2. Total energy of the $S\bar{S}$ system as a function of separation for the configuration HH (dashed line), $x-\pi$ (dash-dotted), and $z-\pi$ (solid) in units of the Skyrme mass. Note the horizontal line is twice the Skyrme mass. The maximum value of the energy at zero separation is four times the Skyrme mass, as we derived in the analytical result.

energy is zero. This shows that, even for the artificial case of zero separation, the $S\bar{S}$ energy is very dependent on grooming.

B. $S\bar{S}$ at a separation and a relative grooming

We now study, in the product ansatz, the energy of the $S\bar{S}$ system as a function of the separation and relative grooming. This can only be done numerically. We now use the full Lagrangian including the finite pion mass term. We put the S and \bar{S} on a 3D lattice with the two solitons a distance R apart on the x axis. The product ansatz is

$$U_{\text{PA}}(\mathbf{r}) = U\left(\mathbf{r} - \frac{R\hat{x}}{2}\right) C U^\dagger\left(\mathbf{r} + \frac{R\hat{x}}{2}\right) C^\dagger, \quad (9)$$

where $U(\mathbf{r})$ is the $SU(2)$ field for a single Skyrmion and C is the grooming matrix. In Skyrme units for length ($1/e f_\pi = 0.45$ fm), the spatial extension of lattice we use is $20 \times 10 \times 10$. We evaluate the derivatives of the U field by the two-point difference:

$$\nabla_i U = \frac{1}{2h} [U(\mathbf{r} + h\mathbf{e}_i) - U(\mathbf{r} - h\mathbf{e}_i)]. \quad (10)$$

With $64 \times 32 \times 32$ points on the lattice and $h = 0.001$, we find that, for large separations, the total energy is within one percent of twice the single Skyrme mass. We calculate the energy for three interesting configurations: (1) no grooming (HH), (2) relative rotation of π around x axis ($x-\pi$), and (3) relative rotation of π around z axis ($z-\pi$). The results are shown in Fig. 2. Recall that the separation is along the x axis.

It is instructive to compare the energy of the $S\bar{S}$ system with the corresponding result for the SS system [5–7]. The $z-\pi$ grooming is the most attractive configuration for SS , while it is the most repulsive for $S\bar{S}$. The $x-\pi$ grooming, while being the most repulsive for SS , is mildly attractive for

$S\bar{S}$. Finally the ungroomed case is the most attractive for $S\bar{S}$ while it is mildly repulsive for SS . This also leads to speculation about the speed of annihilation. In the calculation of [9], the starting configuration is ungroomed and annihilation happens very fast. This may reflect the fact that this is the most attractive channel. The physical nucleon is a linear superposition of groomed Skyrmions and perhaps in this case annihilation will proceed slower than that seen in [9].

C. Expansion of the $S\bar{S}$ energy in the relative grooming variables

We now turn to an expansion of the energy in the relative grooming variables as a first step in obtaining the projection of the $S\bar{S}$ interaction onto the $N\bar{N}$ interaction. We follow the methods developed for obtaining the NN interaction from the SS . As in the calculation of [6,19] for SS , the energy for $S\bar{S}$ can be expanded in the variables c_4 and $\mathbf{c} \cdot \hat{\mathbf{R}}$, with the relative grooming matrix $C = c_4 + i\boldsymbol{\tau} \cdot \mathbf{c}$ and \mathbf{R} the vector connecting the centers of the two solitons. For the SS , the full expansion is

$$V(\mathbf{R}, C) = V_1 + V_2 c_4^2 + V_3 (\mathbf{c} \cdot \hat{\mathbf{R}})^2 + V_4 c_4^4 + V_5 c_4^2 (\mathbf{c} \cdot \hat{\mathbf{R}})^2 + V_6 (\mathbf{c} \cdot \hat{\mathbf{R}})^4, \quad (11)$$

where V_i , $i = 1 - 6$ are functions of R . For $S\bar{S}$, the symmetry of $\mathbf{R} \rightarrow -\mathbf{R}$ is broken by the product ansatz and we need three additional terms for a consistent expansion

$$V_{S\bar{S}} = V(\mathbf{R}, C) + V_7 c_4 (\mathbf{c} \cdot \hat{\mathbf{R}}) + V_8 c_4^3 (\mathbf{c} \cdot \hat{\mathbf{R}}) + V_9 c_4 (\mathbf{c} \cdot \hat{\mathbf{R}})^3. \quad (12)$$

These terms odd in \mathbf{R} are an artifact of the asymmetry of the product ansatz and should be discarded. One can use the symmetrized energy $(V_{S\bar{S}} + V_{\bar{S}S})/2$ to extract V_1 to V_6 , since the V_7 to V_9 terms drop out in this combination.

The six terms in (11) can be expressed in terms of operators in the baryon space using the algebraic methods introduced in [19]. One quantizes each Skyrmion with a $u(4)$ algebra and then the relevant operators and baryon states are easily constructed in terms of the operators of those algebras. The method was developed in [19] for the NN system, but since each Skyrmion gets its own algebra, the method can be taken over without alteration to the $N\bar{N}$ system. The SS or $S\bar{S}$ interaction can be expanded in terms of three operators, the identity and the operators W and Z given by

$$W = T_{pi}^\alpha T_{pi}^\beta / N_C^2, \quad Z = T_{pi}^\alpha T_{pj}^\beta [3\hat{R}_i \hat{R}_j - \delta_{ij}] / N_C^2. \quad (13)$$

Here α and β label the two different set of bosons, used to realize the $u(4)$ algebras. T is a one-body operator with spin 1 and isospin 1. The semiclassical (large- N_C) limit of these operators can be given in terms of \mathbf{R} and C as [19]

$$W_{\text{cl}} = 3c_4^2 - \mathbf{c}^2, \quad Z_{\text{cl}} = 6\mathbf{c} \cdot \hat{\mathbf{R}} - 2\mathbf{c}^2. \quad (14)$$

We can therefore expand the interaction in W and Z , as an alternative to Eq. (11),

$$V(\mathbf{R}, C) = v_1(R) + v_2(R)W_{cl} + v_3(R)Z_{cl} + v_4(R)W_{cl}^2 + v_5(R)W_{cl}Z_{cl} + v_6(R)Z_{cl}^2. \quad (15)$$

The relations between V_i and v_i can be found in Eq. (24) of [19]. The advantage of the algebraic method is it allows us to study both the large N_C limit, and to include finite N_C effects explicitly in a systematic way. It also makes taking baryon matrix elements quite easy. As in the SS case, we find for $S\bar{S}$ that the terms quadratic in Z and W are quite small, and so we neglect them. Hence we can write

$$V = v_1 + v_2W + v_3Z. \quad (16)$$

We can use the algebraic methods of [19] to take the $N\bar{N}$ matrix element of our interaction. Keeping only the leading terms we find

$$V = V_c + V_s(\boldsymbol{\sigma}_1 \cdot \boldsymbol{\sigma}_2)(\boldsymbol{\tau}_1 \cdot \boldsymbol{\tau}_2) + V_t[3(\boldsymbol{\sigma}_1 \cdot \hat{\mathbf{R}})(\boldsymbol{\sigma}_2 \cdot \hat{\mathbf{R}}) - \boldsymbol{\sigma}_1 \cdot \boldsymbol{\sigma}_2] \times (\boldsymbol{\tau}_1 \cdot \boldsymbol{\tau}_2), \quad (17)$$

with

$$V_c = v_1, \quad V_s = \frac{v_2 P_N^2}{9}, \quad V_t = \frac{v_3 P_N^2}{9}. \quad (18)$$

Here P_N is a finite N_C correction factor, $P_N = 1 + 2/N_C$. This gives the nucleons only projection of the $S\bar{S}$ interaction. To obtain the full phenomenological interaction it is necessary to include the effects of Δ and $\bar{\Delta}$ admixtures that become important as the baryons approach each other. We now turn to those admixtures.

III. ADIABATIC INTERACTION

The $N\bar{N}$ potential in Eq. (17) is calculated by projecting Eq. (16) to the nucleon degrees of freedom only. This is certainly the correct procedure for large separation. How-

ever, as the Skyrmion and anti-Skyrmion approach, they can deform. In terms of the baryon degrees of freedom and for $N_C=3$ that means excitation of the Δ and $\bar{\Delta}$ intermediate states. All that is required to define a $N\bar{N}$ interaction is that the particles be $N\bar{N}$ asymptotically. They may deform or excite as they wish as they interact. In the NN case we saw that this intermediate excitation plays a significant role in the intermediate range attraction [8]. For neutral atoms, a corresponding virtual excitation process leads to the attractive Van der Waals force at large distance. For Skyrmions, beside this state mixing, there is a dynamical distortion that goes beyond the product ansatz. This is a crucial part of the NN interaction [14], but the corresponding $S\bar{S}$ distortion is beyond the scope of this paper. For the NN system this distortion, coupled with the state mixing, is crucial for getting the midrange attraction. For the nucleon-antinucleon system we expect similar enhancements of attraction coming from the distortion. The effects of distortion and state mixing both come in at distances where the product ansatz can be expected to fail. Thus our short and midrange results with the product ansatz, even including state mixing, should be taken as only indicative and not as the final word. Further more omega meson exchange is attractive in the $N\bar{N}$ system due to G parity and hence a complete treatment of the $N\bar{N}$ central attraction should extend the Skyrme model to include vector mesons [20].

As in the NN system, we first study the effect of mixing Δ and $\bar{\Delta}$ on the energy perturbatively and then use the Born-Oppenheimer method to consider the effect exactly in the limited subspace.

A. Perturbation theory

We first include the effects of the intermediate states, $N\bar{\Delta}$, $\Delta\bar{N}$, and $\Delta\bar{\Delta}$, on the nucleon antinucleon potential perturbatively. Since we are using separate $u(4)$ algebras for each Skyrmion, the results for NN in [8] can be carried over to the $N\bar{N}$ problem, with Eq. (15) in [8] being the perturbation correction

$$V_{PT}^{(1)} = -\frac{Q_N^2}{\delta} \left\{ \left[\frac{1}{3} Q_N^2 P_0^\tau + \left(\frac{16}{27} P_N^2 + \frac{5}{27} Q_N^2 \right) P_1^\tau \right] (v_2^2 + 2v_3^2) + (\boldsymbol{\sigma}^1 \cdot \boldsymbol{\sigma}^2) \left[-\frac{1}{18} Q_N^2 P_0^\tau + \left(\frac{16}{81} P_N^2 - \frac{5}{162} Q_N^2 \right) P_1^\tau \right] (v_2^2 - v_3^2) \right. \\ \left. + (3\boldsymbol{\sigma}^1 \cdot \hat{\mathbf{R}}\boldsymbol{\sigma}^2 \cdot \hat{\mathbf{R}} - \boldsymbol{\sigma}^1 \cdot \boldsymbol{\sigma}^2) \left[-\frac{1}{18} Q_N^2 P_0^\tau + \left(\frac{16}{81} P_N^2 - \frac{5}{162} Q_N^2 \right) P_1^\tau \right] (v_2^2 - v_2v_3) \right\}. \quad (19)$$

Here δ is the N - Δ mass difference, P_T^τ is a projection operator onto isospin T , and Q_N is another finite N_C correction factor with the value $Q_N = \sqrt{(1-1/N_C)(1+5/N_C)}$. This expresses the leading order correction from state mixing to the $N\bar{N}$ interaction of Eq. (17) in terms of the $S\bar{S}$ terms of Eq. (16). Recall that unlike the work in [8] we are here using the product ansatz to calculate the $S\bar{S}$ interaction rather than a full dynamical scheme.

B. Diagonalization

We now turn to a full diagonalization of the interaction in the $N\bar{N}$, $N\bar{\Delta}$, $\Delta\bar{N}$, and $\Delta\bar{\Delta}$ space. This is the Born-Oppenheimer approximation, and it is valid for $N_C=3$. There are three energy scales or time scales in the problem. The fastest or highest energy scale comes in rearrangements of the pion field itself. These we are modeling using the product ansatz and correspond

to energies on the scale of baryon masses. The intermediate scale is set by the N - Δ energy difference. This is an order $1/N_C$ effect. Finally the $N\bar{N}$ interaction is the smallest energy scale and it is determined by the matrix diagonalization.

We first need the matrix element of the potential Eq. (16) in the space of $N\bar{N}$, $N\bar{\Delta}$, $\Delta\bar{N}$, and $\Delta\bar{\Delta}$ in the angular momentum coupled form. This has been calculated in Eq. (22) of [8] for the baryon-baryon case and the formula remains valid for baryon-antibaryons

$$\begin{aligned} \langle I_1 I_2 L S J T | v | I'_1 I'_2 L' S' J T \rangle &= v_1 \delta_{SS'} \delta_{LL'} \delta_{I_1 I'_1} \delta_{I_2 I'_2} + \frac{v_2}{9} (-1)^{S+T} \delta_{SS'} \delta_{LL'} \begin{Bmatrix} I_1 & I_2 & S \\ I'_2 & I'_1 & 1 \end{Bmatrix} \begin{Bmatrix} I_1 & I_2 & T \\ I'_2 & I'_1 & 1 \end{Bmatrix} \langle I_1 || T^{(11)} || I'_1 \rangle \\ &\times \langle I_2 || T^{(11)} || I'_2 \rangle + \frac{v_3}{9} \sqrt{30} (-1)^{L+L'+S+S'+J+T+I_2+I'_1} \hat{L} \hat{L}' \hat{S} \hat{S}' \begin{Bmatrix} L & 2 & L' \\ 0 & 0 & 0 \end{Bmatrix} \begin{Bmatrix} S & L & J \\ L' & S' & 2 \end{Bmatrix} \\ &\times \begin{Bmatrix} I_1 & I_2 & S \\ I'_2 & I'_1 & 1 \end{Bmatrix} \begin{Bmatrix} I_1 & I_2 & T \\ I'_2 & I'_1 & 1 \end{Bmatrix} \begin{Bmatrix} I_1 & I_2 & S \\ I'_1 & I'_2 & S' \\ 1 & 1 & 2 \end{Bmatrix} \langle I_1 || T^{(11)} || I'_1 \rangle \langle I_2 || T^{(11)} || I'_2 \rangle. \end{aligned} \quad (20)$$

Here I_1 and I_2 are the isospin of the baryon 1 and 2 and T the total isospin. L is the total orbital angular momentum, S is the total spin, and J is, of course, the total angular momentum. The relevant reduced matrix elements are

$$\langle N || T^{(11)} || N \rangle = -10, \quad (21)$$

$$\langle \Delta || T^{(11)} || \Delta \rangle = -20, \quad (22)$$

$$\langle N || T^{(11)} || \Delta \rangle = -8\sqrt{2}. \quad (23)$$

The matrix elements of the kinetic part are taken to be very simple,

$$\begin{aligned} \langle I_1 I_2 L S J T | K | I'_1 I'_2 L' S' J T \rangle \\ = \delta_{I_1 I'_1} \delta_{I_2 I'_2} \delta_{LL'} \delta_{SS'} \left(\delta [I_1 + I_2 - 1] + \frac{L(L+1)}{2M_{I_1 I_2} R^2} \right). \end{aligned} \quad (24)$$

Here $M_{I_1 I_2}$ is the reduced mass, $M_{I_1} M_{I_2} / (M_{I_1} + M_{I_2})$, with $M_{1/2} = 932$ MeV and $M_{3/2} = 1232$ MeV. The mass difference is $\delta M = M_{3/2} - M_{1/2}$.

For the purpose of comparison, we parametrize the full $N\bar{N}$ interaction by

$$V_{NN}^T = V_c^T + V_s^T \boldsymbol{\sigma}^1 \cdot \boldsymbol{\sigma}^2 + V_t^T \sigma_i^1 \sigma_j^2 (3\hat{R}_i \hat{R}_j - \delta_{ij}). \quad (25)$$

The potentials have explicit isospin dependence due to the mixing with states of Δ . To determine the adiabatic potential for $N\bar{N}$, we start at large R where we have nucleons only. As we move to smaller distance, we diagonalize the $K+V$ matrix and follow continuously the eigenvalue corresponding to the $N\bar{N}$ channel. We then subtract the expectation value of K to obtain the adiabatic interaction energy as a function of R .

We first consider the case $T=0$. For $J^\pi=0^-$ (note that nucleon and antinucleon have opposite intrinsic parity), we have three channels $|N\bar{N}L=0 S=0\rangle$, $|\Delta\bar{\Delta}L=0 S=0\rangle$, and $|\Delta\bar{\Delta}L=2 S=2\rangle$. The lowest eigenvalue of the Hamiltonian $K+V$ should be identified with

$$\langle L=0 S=0 | V_{NN}^{T=0} | L=0 S=0 \rangle = V_c^0 - 3V_s^0. \quad (26)$$

For $J^\pi=0^+$, there are three channels $|N\bar{N}L=1 S=1\rangle$, $|\Delta\bar{\Delta}L=1 S=1\rangle$, and $|\Delta\bar{\Delta}L=3 S=3\rangle$. The lowest eigenvalue should be equated to

$$\langle L=0 S=0 | V_{NN}^{T=0} | L=0 S=0 \rangle = V_c^0 + V_s^0 - 4V_t^0. \quad (27)$$

We consider one more set of states with $J^\pi=1^-$ and there are six channels: $|N\bar{N}L=0 S=1\rangle$, $|N\bar{N}L=2 S=1\rangle$, $|\Delta\bar{\Delta}01\rangle$, $|\Delta\bar{\Delta}21\rangle$, $|\Delta\bar{\Delta}23\rangle$, and $|\Delta\bar{\Delta}43\rangle$. The matrix element to identify the lowest eigenvalue with is

$$\langle L=0 S=1 | V_{NN}^{T=0} | L=0 S=1 \rangle = V_c^0 + V_s^0. \quad (28)$$

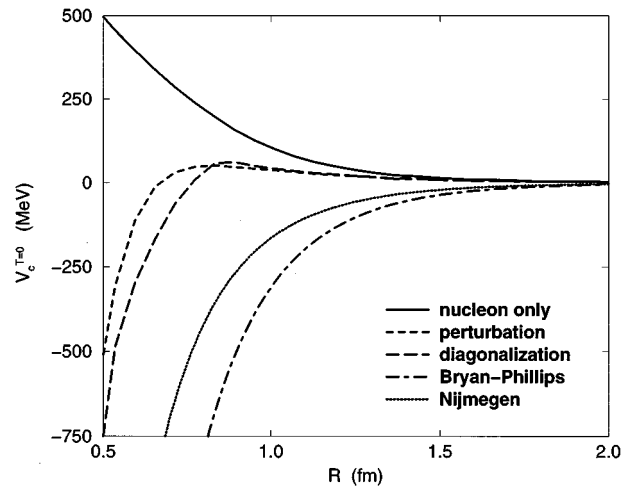


FIG. 3. Central potential V_c^T as a function of R in the region 0.5–2 fm for the $T=0$ channels. The solid line gives the nucleons-only result from the product ansatz. The short-dashed line is the result of the state mixing in perturbation theory and the long-dashed line of the full Born-Oppenheimer diagonalization. The meson exchange potentials are shown by the dash-dotted line for Bryan-Phillips potential [21] and by the dotted line for the Nijmegen potential [22].

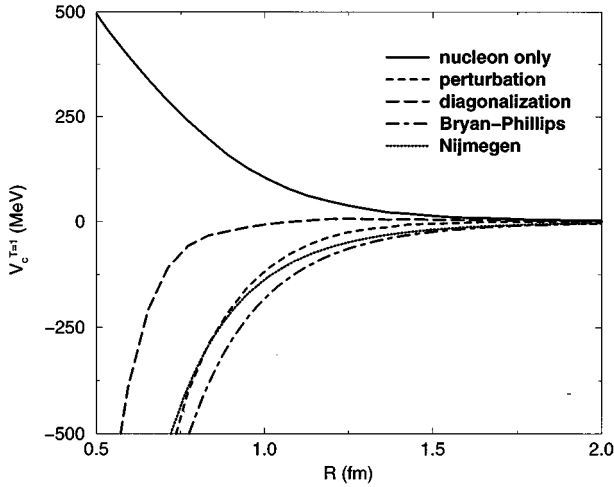


FIG. 4. Central potential, same as in Fig. 3 but for $T=1$.

From these three linear combinations of V_c , V_s , and V_t in Eq. (26) to Eq. (28), the potentials in Eq. (25) are easily solved for $T=0$. A similar calculation applies for $T=1$, except that now $N\bar{\Delta}$ and $\Delta\bar{N}$ channels also appear.

IV. RESULT AND DISCUSSION

For each total isospin $T=0$ and 1, we calculate V_c^T , V_s^T , and V_t^T in Eq. (25) as outlined in the last section. We then compare these results with the phenomenological potentials of Brian-Phillips [21] and of the Nijmegen [22] group. These are potentials based on meson exchange at large distances and phenomenology, including an absorptive part to model annihilation, at small distances. (There have been more recent attempts to describe more $NN\bar{N}$ data coming mainly from LEAR at CERN. These include the the work of the Paris group [23], the Nijmegen group [24], and the Julich group [25]. The $NN\bar{N}$ potentials from these efforts describe more detailed observables, such as differential cross section and polarization. However, they are not so qualitatively different from older ones and we have not included them in our study.) The meson exchange part of these potentials for $NN\bar{N}$ is obtained from the corresponding NN potentials by G -parity transform—the contribution of a particular meson for $NN\bar{N}$ is equal to its part in V_{NN} multiplied by the meson's G parity. We only compare with the scalar, tensor, and spin-spin parts of the potentials. The spin-orbit force is of higher order in $1/N_C$ and we have not calculated it in the Skyrme picture. We should note that various cutoffs are used in the Brian-Phillips, Nijmegen, and other similar potentials. As a result at distance 1 fm or less the strength of the potentials can be significantly different from their meson exchange value. In addition, at distance less than 1 fm, the interaction is dominated by the absorptive potential of order 1 GeV. Furthermore, at these short distances the entire static Skyrme approach, to say nothing of the product ansatz, is no longer meaningful. Hence we should not place any faith on comparisons of our results with the phenomenological potentials around 1 fm or less. At intermediate distances, between 1 fm and 2 fm, the results from our Skyrme approach to the NN interaction suggest that the product ansatz is on the right

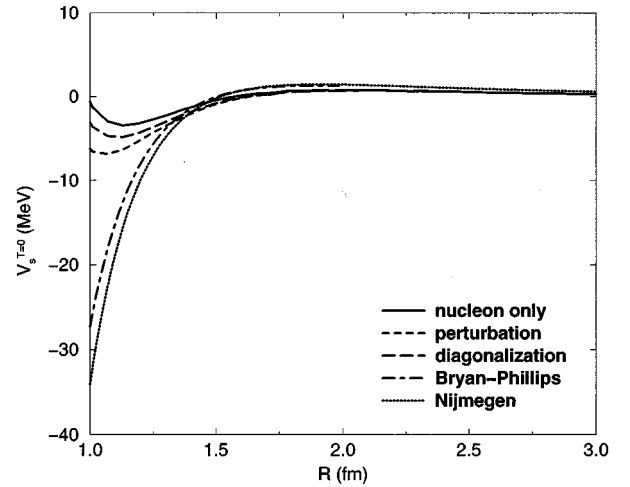


FIG. 5. The spin-dependent potential V_s as a function of R in the region 1–3 fm for $T=0$. Labeling of curves is the same as in Fig. 3.

track, but that careful comparison with phenomenological potentials requires a more complete calculation of the Skyrme dynamics. In particular we expect the product ansatz to underestimate midrange attraction, as it does for NN . This is basically a consequence of the variational theorem. With these thoughts in mind, let us turn to our results.

Figure 3 shows our results for the $T=0$ part of the central potential. We see that the effects of Δ mixing either in perturbation theory or full Born-Oppenheimer diagonalization is significant, but still does not begin to agree with the strong central, midrange attraction seen in the phenomenological potentials. This is the fault of the product ansatz we referred to above. It will be important to see if complete Skyrme calculations can repair this fault. Figure 4 shows the $T=1$ central potential. Here the effects of Δ mixing are more striking since for $T=1$ single Δ intermediate states are permitted. Now we do find some central attraction, but not as much as is seen phenomenologically. Note that where they differ, the full diagonalization result has superior credentials to the perturbation theory result, and it is the diagonalization result

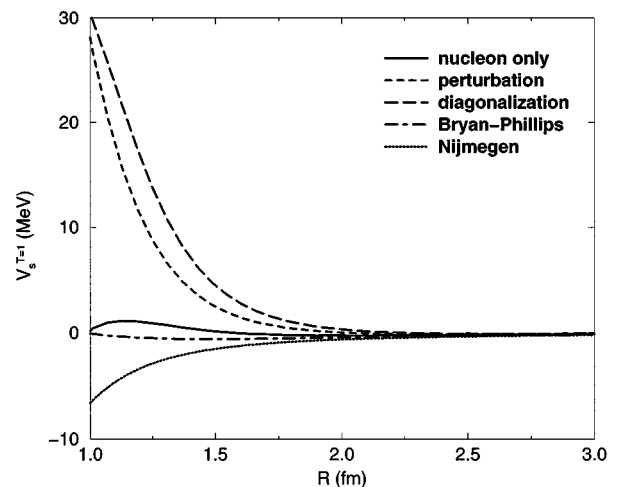


FIG. 6. Spin-dependent potential, same as Fig. 5 but for $T=1$.

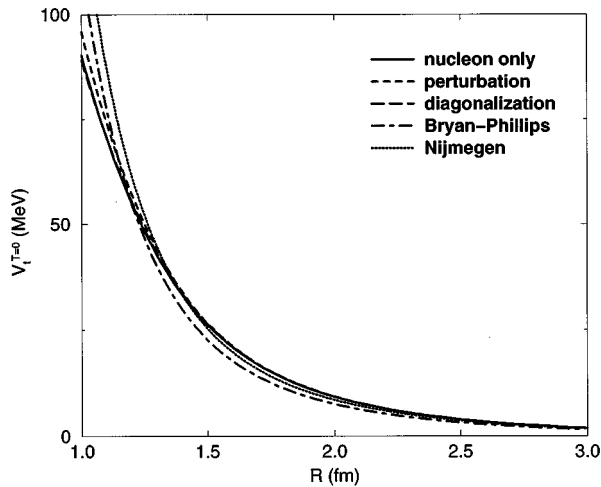


FIG. 7. Tensor potential V_T as a function of R in the region 1–3 fm for $T=0$. Labeling of curves is the same as in Fig. 3.

that is too weak. Again we must await full Skyrme calculation in this channel. Figure 5 shows the $T=0$ spin-spin part of the interaction. Except at the smallest distances, the results are very satisfactory. Note that this is remarkable, since the spin-spin interaction is very weak (note the scale in Fig. 5), and hence arises from cancelation of much larger terms. We believe it is significant that the Skyrme picture can reproduce this scale and even the correct sign. The effects of cancelations are even more striking in Fig. 6 which shows the $T=1$ spin-spin interaction. The corrections from the mixing of delta states are larger than those for $T=0$, since $\bar{N}\Delta$ and $\bar{\Delta}N$ are involved in addition to $\bar{\Delta}\Delta$. Both the perturbative and diagonalization lead to a positive spin-spin potential for $T=1$, in contrast to the negative values in the phenomenological potentials. However, note that even the wrong sign Skyrme results remain really small. Note also that the phenomenological potentials are consistent with zero outside of 1.5 fm. Finally in Figs. 7 and 8 we show the $T=0$ and $T=1$ tensor potentials. All calculations of these agree since they are dominated by one-pion exchange. (Recall that the

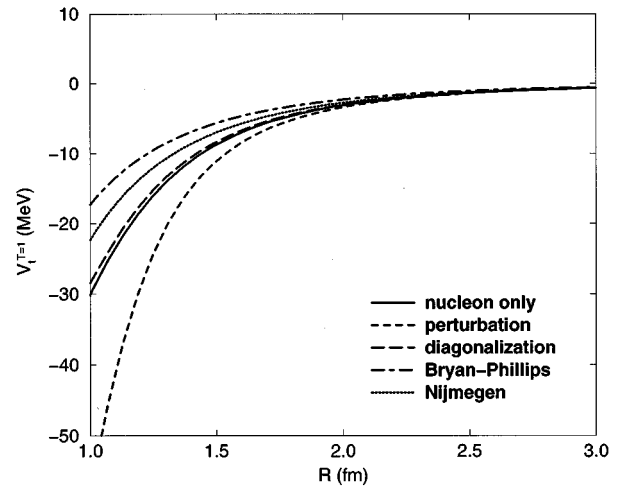


FIG. 8. Tensor potential, same as in Fig. 7 but for $T=1$.

Skyrme picture in the product ansatz gets one pion exchange right.) Hence except for the central attraction, the product ansatz gives a credible account of the nucleon-antinucleon potential, and we understand how the product ansatz fails for the central attraction. Note that there are no free parameters on our calculation.

We have shown that the Skyrme picture with the product ansatz is a reasonable first step to obtaining the real part of the nucleon-antinucleon interaction. We also understand how doing the Skyrme dynamics better can repair the lack of central attraction we find here. Hence the next step is to do that dynamics. Then combining this picture of nucleon-antinucleon interactions in the entrance channel based on the Skyrme model with our previous work on annihilation channels described by this model, we hope to have a unified picture of annihilation based on the large N_C , QCD inspired Skyrme picture.

ACKNOWLEDGMENT

This work was supported in part by a grant from the National Science Foundation.

-
- [1] T.H.R. Skyrme, Proc. R. Soc. London **262**, 237 (1961); Nucl. Phys. **31**, 556 (1962).
 - [2] G. 't Hooft, Nucl. Phys. **B72**, 461 (1974); **B75**, 461 (1974).
 - [3] E. Witten, Nucl. Phys. **B223**, 433 (1983).
 - [4] G.S. Adkins, C.R. Nappi, and E. Witten, Nucl. Phys. **B228**, 552 (1983).
 - [5] A. Jackson, A.D. Jackson, and V. Pasquier, Nucl. Phys. **A432**, 567 (1985).
 - [6] R. Vinh Mau, M. Lacombe, B. Loiseau, W.N. Nottingham, and P. Lisboa, Phys. Lett. **150B**, 259 (1985).
 - [7] A. Hosaka, M. Oka, and R.D. Amado, Nucl. Phys. **A530**, 507 (1991).
 - [8] N.R. Walet and R.D. Amado, Phys. Rev. C **47**, 498 (1993).
 - [9] H.M. Sommermann, R. Seki, S. Larson, and S.E. Koonin, Phys. Rev. D **45**, 4303 (1992).
 - [10] B. Shao, N.R. Walet, and R. D. Amado, Phys. Lett. B **303**, 1 (1991).
 - [11] R.D. Amado, R. Cannata, J-P. Dedonder, M.P. Locher, and B. Shao, Phys. Rev. Lett. **72**, 970 (1994); Phys. Rev. C **50**, 640 (1994).
 - [12] Yang Lu and R.D. Amado, Phys. Lett. B **357**, 446 (1995); Phys. Rev. C **52**, 2158 (1995).
 - [13] M.M. Musakhanov and I.V. Musatov, Phys. Lett. B **273**, 309 (1991).
 - [14] T.S. Walhout and J. Wambach, Phys. Rev. Lett. **67**, 314 (1991).
 - [15] W.Y. Crutchfield and J.B. Bell, J. Comput. Phys. **110**, 234 (1994).
 - [16] A. Depace, H. Mütter, and A. Faessler, Phys. Lett. B **188**, 307 (1987); G. Kälbermann and J.M. Eisenberg, J. Phys. G **15**, 157 (1989).

- [17] D.O. Riska and K. Dannbom, Phys. Scr. **37**, 7 (1988).
- [18] T. Otofujii, S. Sato, M. Yasuno, H. Hanada, and R. Seki, Phys. Lett. B **205**, 145 (1988).
- [19] M. Oka, R. Bijker, A. Bulgac, and R.D. Amado, Phys. Rev. C **36**, 1727 (1987).
- [20] G.S. Adkins and C. R. Nappi, Phys. Lett. **137**, 251 (1984).
- [21] R.A. Brian and R.J.N. Phillips, Nucl. Phys. **B5**, 201 (1968).
- [22] M.M. Nagels *et al.*, Phys. Rev. D **12**, 744 (1975); P.H. Timmers *et al.*, Phys. Rev. D **29**, 1928 (1984).
- [23] M. Pignone, M. Lacombe, B. Loiseau, and R. Vinh Mau, Phys. Rev. C **50**, 2710 (1994).
- [24] R. Timmermans, T.A. Rijken, and J.J. de Swart, Phys. Rev. C **50**, 48 (1994).
- [25] T. Hippchen, J. Haidenbauer, K. Holinde, and V. Mull, Phys. Rev. C **44**, 1323 (1991).